Nanoscale Advances

ROYAL SOCIETY OF CHEMISTRY

COMMUNICATION

View Article Online
View Journal | View Issue

Cite this: *Nanoscale Adv.*, 2021, **3**, 2475

Wearable and washable light/thermal emitting textiles†

Zhihui Tian,‡[a] Heshan Zhang,‡[a] Fei Xiu,*[a] Minjie Zhang,[a] Jiahao Zou,[a] Chaoyi Ban,[a] Yijie Nie,[a] Wenjie Jiang,[a] Bin Hu[b] and Juqing Liu *[a]

Received 22nd January 2021
Accepted 19th March 2021

DOI: 10.1039/d1na00063b

rsc.li/nanoscale-advances

Electronic textiles (e-textiles) typically comprise fabric substrates with electronic components capable of heating, sensing, lighting and data storage. In this work, we rationally designed and fabricated anisotropic light/thermal emitting e-textiles with great mechanical stability based on a sandwich-structured tri-electrode device. By coating silver nanowire network/thermal insulation bilayer on fabrics, an anisotropic thermal emitter can be realized for smart heat management. By further covering the emissive film and the top electrode on the bilayer, light emitters with desirable patterns and colors are extracted from the top surface *via* an alternative current derived electroluminescence. Both the light and thermal emitting functions can be operated simultaneously or separately. Particularly, our textiles exhibit reliable heating and lighting performance in water, revealing excellent waterproof feature and washing stability.

Introduction

Developing multifunctional textile is the primary goal of smart cloth for personalized healthcare. Generally, electronic textiles (e-textiles) with personal thermal management (PTM) are recognized as a new effective and energy-saving way to maintain the temperature focusing on the human body.[1–6] A PTM device should assure the basic needs of being wearable, washable,[7,8] and capable of raising the body temperature or cooling if desired.[9] For personal heating, coating conductive nanomaterials on fabrics has been demonstrated to be an effective approach *via* reflecting infrared radiation (IR) back to the human body.[10–12] Typically, silver nanowires (AgNWs) with high IR reflection efficiency and excellent electrical conductivity are the most promising choice among various metallic nanofibers.[13,14] Although e-textiles for PTM have been developed rapidly, functional diversity realized on a single device is highly desirable, which is of great significance for the facile fabrication and long-term operation.

With an increasing demand for intelligent fabrics, the studies on the multifunctionalization of e-textiles have been explored recently. By integrating current electronic or optoelectronic devices, such as nanogenerators,[15] sensors,[16] energy storage[17] or light-emitting devices,[18] with textile substrates, various multifunctionalized e-textiles have been demonstrated.[19,20] For instance, Dong *et al.* reported a series of multifunctional conductive hydrogel/thermochromic elastomer hybrid fibers with core–shell segmental configuration and their application as flexible wearable strain and temperature sensors to monitor human motion and body/surrounding temperatures.[21] Chen *et al.* simultaneously integrated a triboelectric nanogenerator with a light emitting diode (LED) on clothes to achieve lighting driven by the triboelectric nanogenerator.[22] Although multifunctional e-textiles have made great progress, further simplification of the preparation process as well as the circuit structure is in urgent need. Especially, intrinsically producing all-in-one wearable electronics with satisfying multiparameter management is still challenging.

Herein, we report washable multifunctional e-textiles based on a sandwich-structured tri-electrode device. Tunable heating effect could be realized by depositing a conductive AgNW film on the fabric for efficient heat management. By covering the thermal insulation film, the emissive layer and the top electrode on the surface of the AgNW film, anisotropic thermal regulation and light emission could be achieved simultaneously or separately on a single device. Particularly, the fabricated e-textiles exhibited excellent waterproof features and washing stability, benefiting from all the materials involved in the textile device being waterproof, endowing them with excellent application potential in smart wearable electronics.

[a]*Key Laboratory of Flexible Electronics (KLOFE) & Institute of Advanced Materials (IAM), Nanjing Tech University (NanjingTech), 30 South Puzhu Road, Nanjing, 211816, China. E-mail: iamfxiu@njtech.edu.cn; iamjqliu@njtech.edu.cn*

[b]*School of Optics and Photonics, Beijing Institute of Technology, Beijing, 100081, China*

† Electronic supplementary information (ESI) available. See 10.1039/d1na00063b

‡ Z. H. T. and H. S. Z. contributed equally to this work.

Experimental

Materials

A commercially available cotton textile was used as the substrate. Norland optical adhesive (NOA63) and ethanol were purchased from Aladdin Chemicals. Cesium tungsten bronze was purchased from Shunfeng Nano Technology Co., Ltd. AgNWs were synthesized according to the previously reported work.[23] The morphology of the AgNWs is characterized and shown in Fig. S1 (ESI†), and the average length and diameter of the silver nanowire is 9 μm and 28 nm, respectively. ZnS : Cu, ZnS : Cu, Mn phosphors and PB were purchased from Shanghai KPT Co. Water (18.2 MΩ cm) was purified using a Milli-Q purification system (DZG-303A).

Preparation of AgNW–polymer–fabric electrodes

AgNWs were dispersed in ethanol and then deposited onto a pre-cleaned plastic Petri dish substrate by spray coating on a 50 °C hot plate with a rectangle shadow mask. The NOA63 solution was poured into the plastic Petri dish, then covered with a piece of fabric and cured by UV light. Next, the AgNW–NOA63–fabric electrode was peeled off from the plastic substrate and fixed with a tape for further fabrication.

Fabrication of the dual-mode electronic textile device

A mixed solution of PB (5 g) and ZnS : Cu (5 g) as the emitter was prepared for the blue light emitting material, and a solution of ZnS : Cu, Mn (5 g) and PB (5 g) was prepared for the yellow light emitting material. The white light emitting material was prepared by mixing ZnS : Cu (2 g), ZnS : Cu, Mn (3 g) and PB (5 g), and their emission spectra are shown in Fig. S2 (ESI†). Fig. S2(d)–(f)† show the CIE chromaticity diagrams with color coordinates for all of the light emitting materials. As expected from the EL results, their CIE coordinates ($x = 0.1636$, $y = 0.1728$), ($x = 0.5122$, $y = 0.4636$) and ($x = 0.3042$, $y = 0.2917$) were within the blue region, yellow region and white region, respectively. Next, the mixed solution was spun coated onto a AgNW–polymer electrode at a spinning rate of 3000 rpm for 50 s and cured at 60 °C for 2 h. In addition, the composition of the light-emitting layer was confirmed by X-ray diffraction (XRD) shown in Fig. S3 (ESI†). Then, AgNWs were spray-coated onto the emission layer on a 50 °C hot plate with a rectangle shadow mask. Finally, the device was dried and encapsulated with a thin NOA63 layer to protect the device.

Characterization

The sheet resistance was measured by using a standard four-point probe technology (ST2253 was purchased from Suzhou Jingge Electronic Co.). The device in the lighting mode was powered by AC power (AN97000H was purchased from Ainuo Instrument Co., Ltd), and the luminance of the device was measured by using a spectrophotometer PR745 (6745-1001-00). The device in the heating mode was powered by DC power (RXN-605D was purchased from Zhaoxin Electronic Equipment Co., Ltd.). All thermal images were taken by using an infrared camera (FLIR Ti100). All electrical measurements were carried out in an ambient air environment.

Results and discussion

Fig. 1 demonstrates the application concept and the working principle of the wearable electronic textile device with a vertically stacked sandwich structure consisting of AgNW–polymer electrodes and ZnS–polymer emissive layer. The cross-sectional scanning electron microscopic (SEM) image of the device is shown in Fig. S4 (ESI†). The SEM image showed that the thickness of the thermal insulation layer, the luminous layer

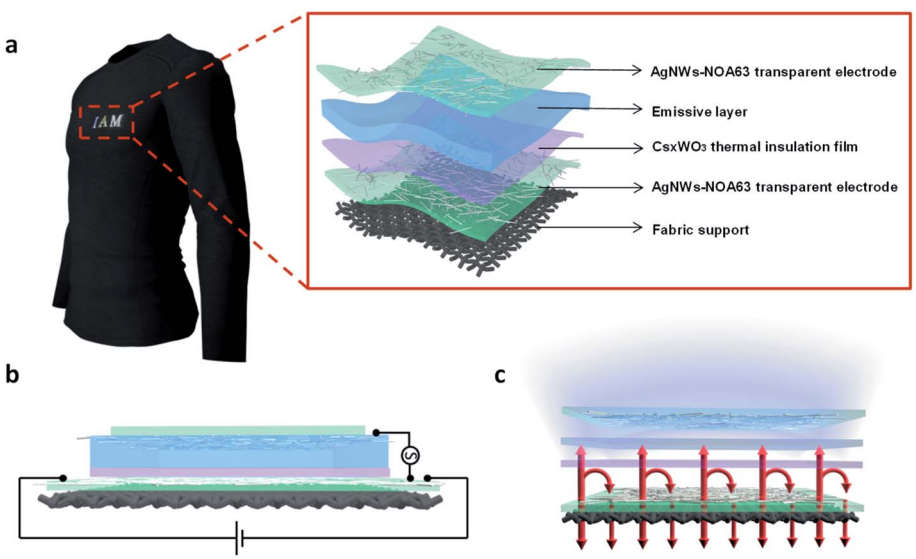

Fig. 1 (a) Schematic illustration of the wearable textile device with lighting and heating dual-functions. (b) Schematic diagram of the device structure and working principle of the dual-mode operation. (c) Working principle of the dual-mode device with directed thermal management and light emission.

and the NOA63 protective layer were about 4 μm, 12 μm and 6 μm, respectively. The tunable heating effect was realized by coating conductive AgNW film on the fabric due to the generation of joule heat when a direct current (DC) voltage was applied on the bottom electrode (Fig. 1b).[24,25] By subsequently covering the thermal insulation film, the emissive layer and the top electrode on the surface of the AgNW film, the tunable light emission could be achieved by applying an alternating current (AC) between the top and the bottom electrodes (Fig. 1b). These two functions exhibited by the fabric device suggested a smart application in functional fabrics. To guarantee an efficient and directed thermal management, a layer of cesium tungsten bronze (Cs_xWO_3) as the thermal insulation film was incorporated between the AgNW–NOA63 heating film and the light-emitting layer to reduce any unnecessary heat loss due to external environment and maintain the temperature focusing on the human body (Fig. 1c).[26,27]

To explore the electrical heating performance of the dual-mode device, the time-dependent temperature profiles of the AgNW–NOA63 film ($R_S \approx 12\ \Omega\ sq^{-1}$) under applied voltages in a range of 1.0–3.0 V were investigated. Fig. 2a shows that the device demonstrates almost the same fast response time under three different applied voltages and reaches a saturation temperature within 70 seconds. As the applied voltage increased from 1.0 to 3.0 V, the saturation temperature increased from 37 °C to 81 °C, suggesting an obvious voltage-dependent

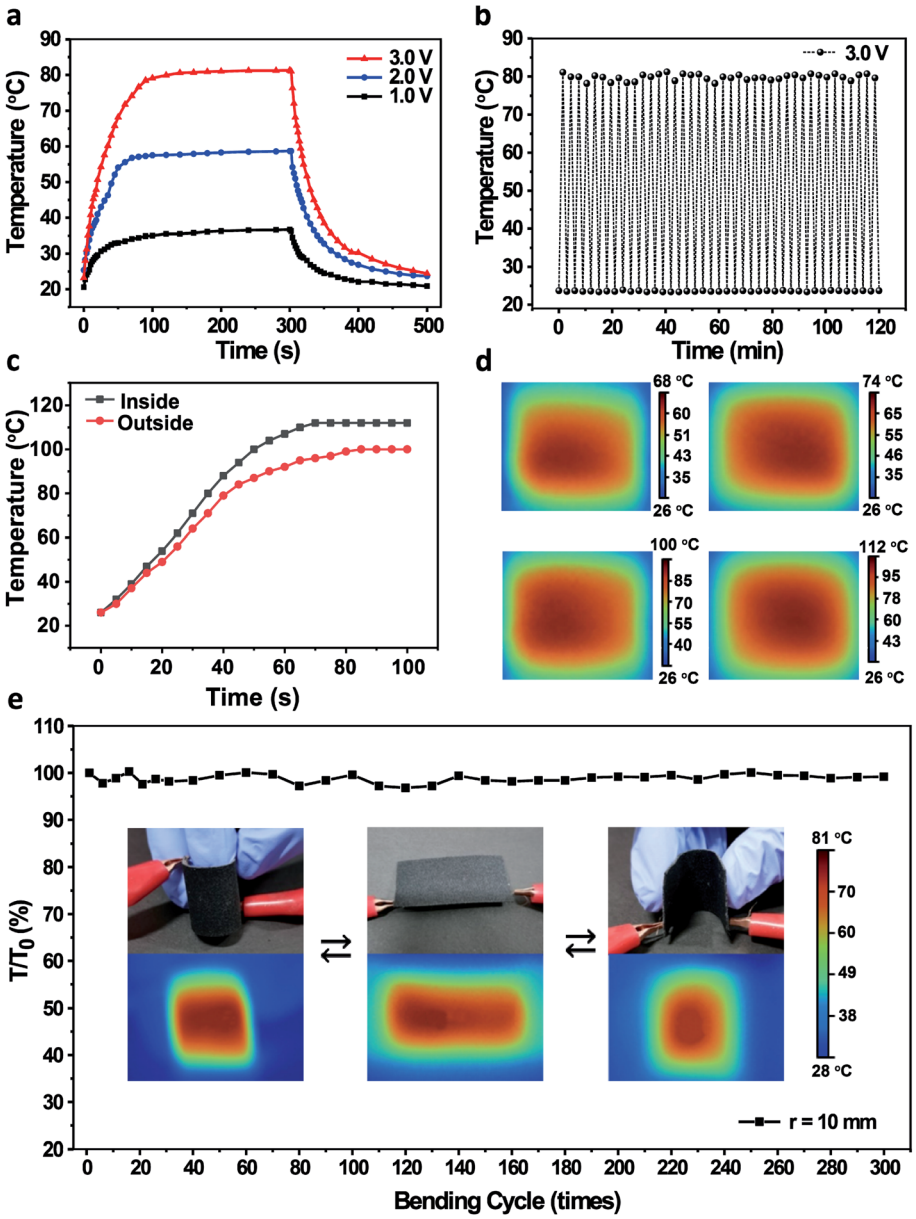

Fig. 2 (a) Time-dependent surface temperature profiles of a AgNW–NOA63 film heater ($R_S \approx 12\ \Omega\ sq^{-1}$) at different input voltages. (b) Cyclic on–off test results for the AgNW–NOA63 film heater. (c) Function of the temperature on both sides of the insulation film. (d) Infrared photographs of the heater on both sides of the thermal insulation film. (e) Temperature of the heater as a function of the bending cycle.

heating property.[28] Fig. 2b shows a fast thermal response behavior of the device, and the saturation temperature and response time of the device exhibit almost no evident decline during the 40 repeated heating/cooling cycles with durations of ~3 min under an input voltage of 3.0 V, indicating a high heating stability of the device. Fig. 2c, d show that the inside temperature of the device is clearly higher than that of the outside, benefiting from the Cs_xWO_3 thermal insulation film. Moreover, bending tests with 300 repeated cycles of two-side bending and release process were carried out to further study the heating reliability of the device. Fig. 2e shows that the heating performance of the device remains stable over 300 bending cycles, confirming the excellent long-term heating reliability of the device due to the embedding of AgNWs.

Besides the outstanding electrical heating performance, the as-fabricated electronic textile device also demonstrated an excellent light emission property. The as-fabricated fabric device demonstrated a bright and uniform light emission powered by an alternating current bias and enabled excellent mechanical flexibility (Fig. 3a). Fig. 3b shows that the fabric device exhibits a very stable and constant real-time luminance upon repeated bending with a radius of curvature of 20 mm, suggesting excellent mechanical stability and luminance stability. Moreover, no obvious change in luminance was observed when the radius of bending curvature was gradually changed, further verifying the satisfactory emission property of the device. Fig. 3c shows that the device begins to emit light at a bias voltage of about 100 V, and the emission intensity increases rapidly thereafter to reach as high as 98 Cd m^{-2} at 300 V and 400 Hz. The relationship between the relative bias voltage and the electroluminescence (EL) intensity could be written as the following formula:[29–31]

$$L = L_0 \exp(-b/V^{1/2}) \quad (1)$$

where L is the brightness, V is the applied voltage, and L_0 and b are constants associated with the device (the particle size of the phosphor, the concentration of the EL powder in the dielectric, the dielectric constant of the embedding medium and the thickness of the emitting layer). Considering the simple device structure, outstanding flexibility and luminance stability, fabric alternating current electroluminescent (ACEL) devices with patterned shapes could be rationally designed and fabricated *via* various approaches. For example, by dipping a pen with ZnS–polymer light-emitting layer and directly writing on AgNW–NOA63–fabric substrate, devices with defined shapes as well as different colors were fabricated (Fig. 3d–f). In addition,

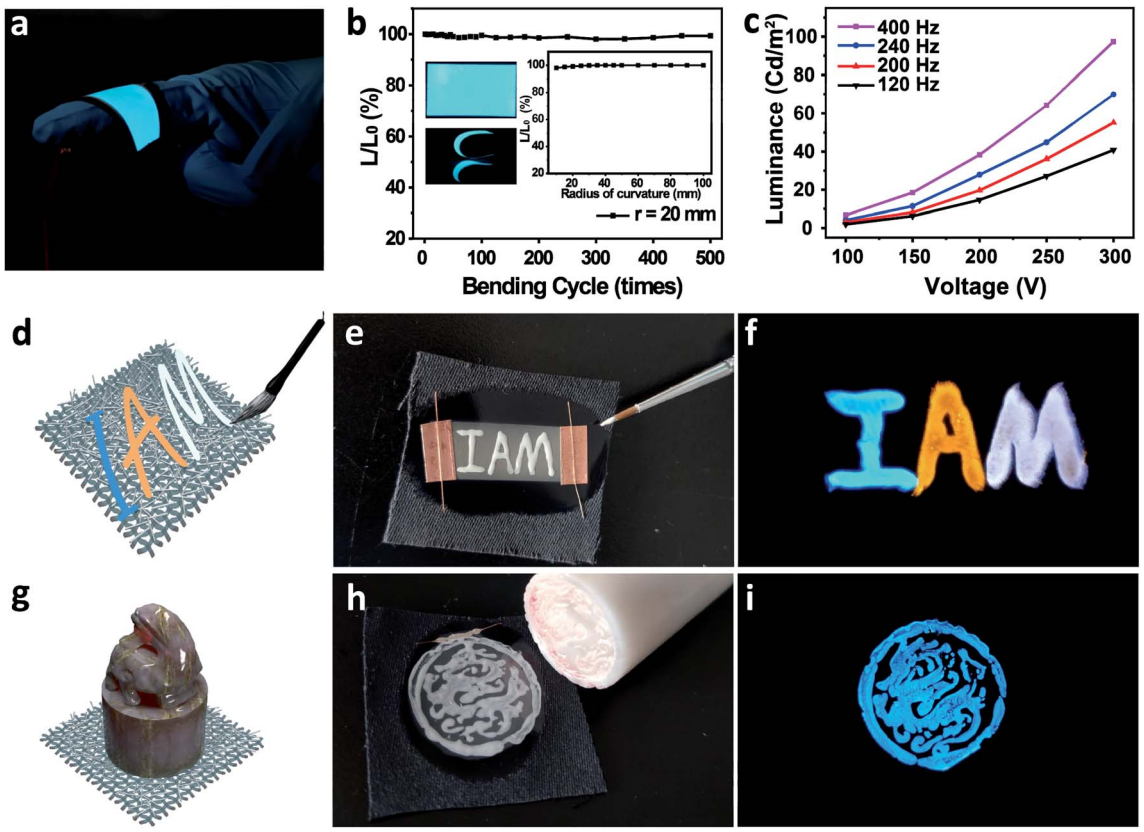

Fig. 3 (a) The flexible lighting device under a mechanically distorted state. (b) The luminance variation of the lighting device under different curvatures and the luminance variation during 500 times bending. (c) Luminance *versus* alternating voltage properties of the device at different frequencies. (d) Schematic diagram of the device patterned by the dipping pen writing. (e) Optical picture of the device patterned by the dipping pen writing. (f) Luminescence picture of the device patterned by the dipping pen writing. (g) Schematic diagram of the device patterned by embossing. (h) Optical picture of the device patterned by embossing. (i) Luminescence picture of the device patterned by embossing.

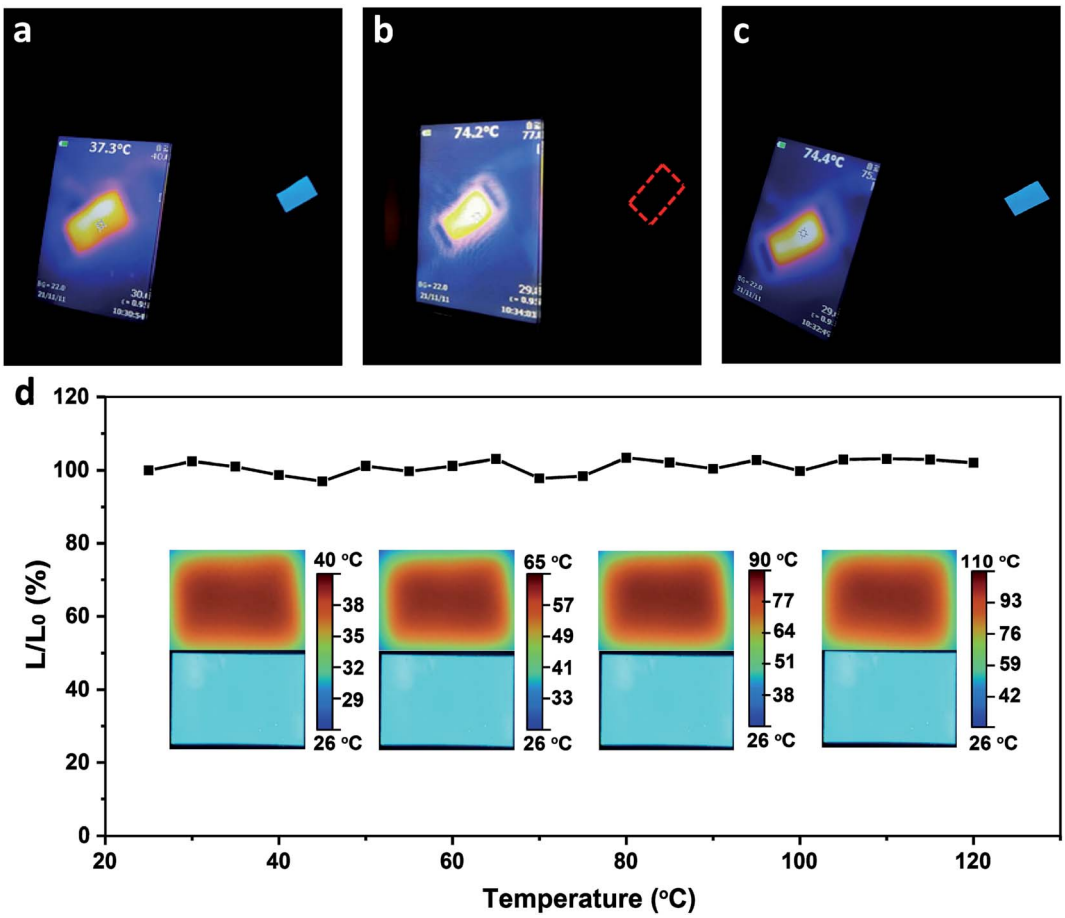

Fig. 4 (a) Photograph of the device in the lighting mode. (b) Photograph of the device in the heating mode. (c) Photograph of the device both in lighting and heating mode simultaneously. (d) The relationship between the heating temperature and the luminance of the device.

flexible devices with more complicated patterns could be obtained by the embossing approach (Fig. 3g–i).

Benefiting from good stability of both heating and lighting performances, these two functions of the device were further investigated. When AC power was applied on the device with a bottom AgNW electrode with a sheet resistance of 13 Ω sq^{-1}, the device was in lighting mode and emitted a bright blue light with a surface temperature of 37 °C (Fig. 4a). In the case of heating mode, when DC power was applied, the device emitted no light while the temperature increased to 74 °C (Fig. 4b). If both AC and DC power were applied, the device exhibited a high surface temperature of 74 °C and emitted light (Fig. 4c). These results revealed that the heating and lighting functions of the e-textiles could work separately, and the device could simultaneously achieve a good heating/lighting performance. Fig. 4d shows that the brightness of the device does not change significantly as the surface temperature increases due to an increase in the applied voltage, which confirms that the dual functions perform independently without any effect on each other when working simultaneously.

To explore the washable property of the flexible e-textiles, the heating and lighting performances of the device after washing for 50 cycles were investigated. Fig. 5 shows that the dual-mode

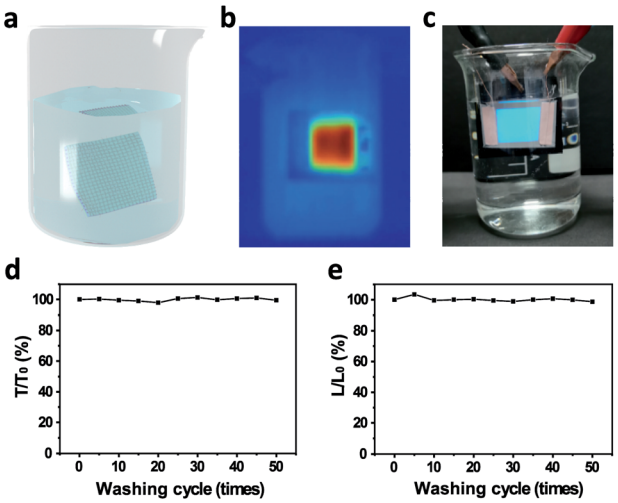

Fig. 5 (a) Schematic diagram of the water-proof property and washability of the device. (b) Infrared photograph of the device in heating mode in water. (c) Photo of the device in lighting mode in water. (d) Heating performance of the device after different washing cycles. (e) Lighting performance of the device after different washing cycles.

device still maintains integrated structure in water and works normally. As the washing time prolonged, the heating temperature and the electroluminescence of the device almost remained unchanged, which suggested an excellent waterproof performance and washing stability of the flexible fabric devices, endowing them with great application potential in functional wearable electronics.

Conclusions

In summary, we present a waterproof and flexible sandwich-structured tri-electrode electronic textile device with lighting and heating dual functions. By coating silver nanowire network/thermal insulation bilayer on fabrics, an anisotropic thermal emitter could be realized for smart heat management with the saturation temperature ranging from 37 °C to 81 °C as the applied voltage was increased from 1.0 to 3.0 V. Particularly, the inside temperature of the device was evidently higher than that of the outside, benefiting from the Cs_xWO_3 thermal insulation film. On the other hand, light emitters with defined patterns and tunable colors ranging from blue, yellow to bright white were extracted from the top surface *via* alternative current-derived electroluminescence. Both the light and thermal emitting functions could be operated simultaneously or separately. Importantly, the washable properties of the e-textiles were studied, and they exhibited stable heating and lighting performances in water, thereby revealing an excellent waterproof feature and washing stability.

Conflicts of interest

There are no conflicts to declare.

Acknowledgements

We thank the primary financial supports from the National Key R&D Program of China (2017YFB1002900), the National Natural Science Foundation of China (61622402), and the Jiangsu Specially-Appointed Professor Programme, the Six Talent Plan (2015XCL015).

Notes and references

1 P.-C. Hsu, A. Y. Song, P. B. Catrysse, C. Liu, Y. Peng, J. Xie, S. Fan and Y. Cui, *Science*, 2016, **353**, 1019–1023.
2 R. Hu, Y. Liu, S. Shin, S. Huang, X. Ren, W. Shu, J. Cheng, G. Tao, W. Xu, R. Chen and X. Luo, *Adv. Energy Mater.*, 2020, **10**, 1903921.
3 Y. Kim, Y. Zhou, S. Schiavon, P. Raftery and G. Brager, *Build. Environ.*, 2018, **129**, 96–106.
4 Y. Peng, J. Chen, A. Y. Song, P. B. Catrysse, P.-C. Hsu, L. Cai, B. LiU, Y. Zhu, G. Zhou, D. S. Wu, H. R. Lee, S. Fan and Y. Cui, *Nature Sustainability*, 2018, **1**, 105–112.
5 K. Qiu, A. Elhassan, T. Tian, X. Yin, J. Yu, Z. Li and B. Ding, *ACS Appl. Mater. Interfaces*, 2020, **12**, 11016–11025.
6 R. Zhou, P. Li, Z. Fan, D. Du and J. Ouyang, *J. Mater. Chem. C*, 2017, **5**, 1544–1551.
7 Y. Guo, C. Dun, J. Xu, J. Mu, P. Li, L. Gu, C. Hou, C. A. Hewitt, Q. Zhang, Y. Li, D. L. Carroll and H. Wang, *Small*, 2017, **13**, 1702645.
8 Y. Wang, L. Chen, H. Cheng, B. Wang, X. Feng, Z. Mao and X. Sui, *Chem. Eng. J.*, 2020, **402**, 126222.
9 P.-C. Hsu, C. Liu, A. Y. Song, Z. Zhang, Y. Peng, J. Xie, K. Liu, C.-L. Wu, P. B. Catrysse, L. Cai, S. Zhai, A. Majumdar, S. Fan and Y. Cui, *Sci. Adv.*, 2017, **3**, e1700895.
10 A. Hazarika, B. K. Deka, D. Kim, H. E. Jeong, Y. B. Park and H. W. Park, *Nano Lett.*, 2018, **18**, 6731–6739.
11 P.-C. Hsu, X. Liu, C. Liu, X. Xie, H. R. Lee, A. J. Welch, T. Zhao and Y. Cui, *Nano Lett.*, 2015, **15**, 365–371.
12 X. Yue, M. He, T. Zhang, D. Yang and F. Qiu, *ACS Appl. Mater. Interfaces*, 2020, **12**, 12285–12293.
13 J. Liang, K. Tong and Q. Pei, *Adv. Mater.*, 2016, **28**, 5986–5996.
14 W. Xiong, H. Liu, Y. Chen, M. Zheng, Y. Zhao, X. Kong, Y. Wang, X. Zhang, X. Kong, P. Wang and L. Jiang, *Adv. Mater.*, 2016, **28**, 7167–7172.
15 K. Dong, X. Peng and Z. L. Wang, *Adv. Mater.*, 2020, **32**, e1902549.
16 M. Lou, I. Abdalla, M. Zhu, J. Yu, Z. Li and B. Ding, *ACS Appl. Mater. Interfaces*, 2020, **12**, 1597–1605.
17 Y. Yang, Q. Huang, L. Niu, D. Wang, C. Yan, Y. She and Z. Zheng, *Adv. Mater.*, 2017, **29**, 1606679.
18 Z. Zhang, K. Guo, Y. Li, X. Li, G. Guan, H. Li, Y. Luo, F. Zhao, Q. Zhang, B. Wei, Q. Pei and H. Peng, *Nat. Photonics*, 2015, **9**, 233–238.
19 H. He, Y. Fu, W. Zang, Q. Wang, L. Xing, Y. Zhang and X. Xue, *Nano Energy*, 2017, **31**, 37–48.
20 X. Pu, W. Song, M. Liu, C. Sun, C. Du, C. Jiang, X. Huang, D. Zou, W. Hu and Z. L. Wang, *Adv. Energy Mater.*, 2016, **6**, 1601048.
21 J. Chen, H. Wen, G. Zhang, F. Lei, Q. Feng, Y. Liu, X. Cao and H. Dong, *ACS Appl. Mater. Interfaces*, 2020, **12**, 7565–7574.
22 C. Chen, H. Guo, L. Chen, Y. C. Wang, X. Pu, W. Yu, F. Wang, Z. Du and Z. L. Wang, *ACS Nano*, 2020, **14**, 4585–4594.
23 Y. Liu, Y. Chen, R. Shi, L. Cao, Z. Wang, T. Sun, J. Lin, J. Liu and W. Huang, *RSC Adv.*, 2017, **7**, 4891–4895.
24 H. Fang, X. Wang, Q. Li, D. Peng, Q. Yan and C. Pan, *Adv. Energy Mater.*, 2016, **6**, 1600829.
25 T. Ye, F. Xiu, S. Cheng, C. Ban, Z. Tian, Y. Chen, Y. Ding, Z. Zhen, J. Liu and W. Huang, *ACS Nano*, 2020, **14**, 6707–6714.
26 L. Peng, W. Chen, B. Su, A. Yu and X. Jiang, *Appl. Surf. Sci.*, 2019, **475**, 325–333.
27 X. Wu, S. Yin, D. Xue, S. Komarneni and T. Sato, *Nanoscale*, 2015, **7**, 17048–17054.
28 T. Kim, Y. W. Kim, H. S. Lee, H. Kim, W. S. Yang and K. S. Suh, *Adv. Funct. Mater.*, 2013, **23**, 1250–1255.
29 Y. Chen, H. Lu, F. Xiu, T. Sun, Y. Ding, J. Liu and W. Huang, *Sci. Rep.*, 2018, **8**, 6408.
30 T. Sun, F. Xiu, Z. Zhou, C. Ban, T. Ye, Y. Ding, J. Liu and W. Huang, *J. Mater. Chem. C*, 2019, **7**, 1472–1476.
31 S. Zhang, R. J. W. Teo, H. Su, C. S. Tan and T. K. S. Wong, *Opt. Mater. Express*, 2016, **6**, 2879–2891.